The Effect of Secondary Refining on the Removal of Phosphorus from Metallurgical-Grade Silicon by Acid Leaching

HAIFEI LU, KUIXIAN WEI, WENHUI MA, KEQIANG XIE, JIJUN WU, and YUN LEI

The effects of structural composition, particle size, leaching time, temperature, and liquid–solid ratio on the removal of phosphorus from metallurgical-grade silicon (MG-Si) by acid leaching were investigated. Two specimens with different phase constitutions were studied: crude metallurgical-grade silicon (C-MG-Si), which is reduced from electric arc furnace, with a high content of Al and Ca, and a secondary refined metallurgical-grade silicon (S-MG-Si) obtained after secondary refining in ladle. Using scanning electron microscopy-energy dispersive spectroscopy, the phosphorus-containing phase was only detected in the C-MG-Si grain boundaries. The Si_2Al_2Ca phase, which was soluble in HCl, showed an affinity for phosphorus, with up to 0.53 wt pct dissolved in this phase. The optimum conditions for acid leaching were grain size, 75-106 μm; leaching time, 6 hours; leaching temperature, 338 K (65 °C); liquid–solid ratio, 6:1; and HCl concentration, 4.0 mol L^{-1}. Using these conditions, the mass fractions of P in C-MG-Si and S-MG-Si were reduced from 105×10^{-6} and 76×10^{-6} to 48×10^{-6} and 61×10^{-6}, respectively, with removal efficiencies of 54.3 and 19.7 pct, respectively. Besides, the investigation suggested that adding HF was beneficial for the removal of most impurities. After 6 hours of leaching MG-Si with a mixture composed of 4.0 mol L^{-1} HCl and 3.0 mol L^{-1} HF, the purity of C-MG-Si and S-MG-Si were increased from 97.55 and 99.31 pct to 99.91 and 99.87 pct, respectively, with extraction efficiencies of 96.14 and 81.59 pct, respectively. The etching results reveal that the HCl-HF mixture was an effective lixiviant for dissolving impurity inclusions in both C-MG-Si and S-MG-Si.

I. INTRODUCTION

WITH the increasing development of the photovoltaic industry, the demand for solar-grade silicon (SOG-Si), as the main material, has increased dramatically. At present, the main preparation technologies for polycrystalline silicon include the modified Siemens process and the fluidized bed reactor process. However, these processes have some disadvantages, such as high-energy consumption and large investment

costs, which has limited the development and application of solar cells. On the other hand, with the advantages of low-energy consumption and environmental friendliness, metallurgical-grade silicon (MG-Si) is widely used to prepare polycrystalline silicon. This process[1–5] comprises secondary refining, acid leaching, vacuum treatment, and directional solidification.

Hydrometallurgy purification, which is the pretreatment process in the metallurgical method, is preliminarily used to purify MG-Si *via* acid leaching. This process has many advantages, including effective removal of impurities, simple equipment, and easy scalability. In 1927, Tucker[6] first proposed the method of acid leaching for purifying pulverized MG-Si. Subsequently, many experiments have been carried out mainly involving the selection of leaching agents, optimization of reaction kinetics, and the enhancement of the leaching process. Hunt *et al.*[7] achieved the removal of more than 90 pct of the impurities in MG-Si by using an average particles size of less than 50 μm and leaching with aqua regia at 348 K (75 °C) for 12 hours. Santos *et al.*[8] have studied acid leaching as a function of the particle size, time, temperature, and concentration

HAIFEI LU and YUN LEI are with the Faculty of Metallurgy and Energy Engineering, Kunming University of Science and Technology, Kunming 690093, People's Republic of China. KUIXIAN WEI and JIJUN WU are with the State Key Laboratory of Complex Nonferrous Metal Resources Cleaning Utilization in Yunnan Province, Kunming University of Science and Technology, Kunming 650093, People's Republic of China. Contact e-mail: kxwei2008@hotmail.com WENHUI MA and KEQIANG XIE are with the National Engineering Laboratory for Vacuum Metallurgy, Faculty of Metallurgical and Energy Engineering, Kunming University of Science and Technology, Kunming 650093, People's Republic of China. Contact e-mail: mwhsilicon@126.com

of leaching agents (HNO_3, H_2SO_4, HCl, and HF). They found that the use of HCl achieved better results than H_2SO_4, HNO_3, or their mixture. Norman et al.[9] demonstrated that upgraded silicon with 99.9 pct purity could be achieved by leaching in three successive steps with aqua regia, HF and HCl, with an average particle size of 100 meshes. Sahu and Asselin[10] investigated the effects of using two different oxidizing agents, such as ferric chloride and ammonium persulfate, on the purification of MG-Si by leaching with HCl. The addition of an oxidizing agent improved the extraction of impurities from the MG-Si. Zeng et al.[11] studied the purification MG-Si by acid leaching with different types of acid, and found an improved effect when using HCl first following by HF. The removal rates of Mg, Al, Ca, Fe, and Ti were 96.8, 96.8, 98.2, 99.7, and 98.0 pct, respectively. Zhang et al.[12] investigated the chemical cracking effect on MG-Si during leaching by aqua regia. They found that the granularity of the particles was reduced by acid leaching, and this phenomenon became more noticeable as the silicon particle size increased. Furthermore, the remarkable removal efficiencies were obtained from the coarse particle size, with removal of 79 pct Fe, 77 pct Al, 45 pct Ca, and 63 pct Ti.

The above studies were mainly aimed at removing metal impurities from MG-Si, as the small segregation coefficient of metallic impurities could facilitate their co-precipitation at the grain boundaries during the solidification process. When MG-Si is pulverized, fractures mainly occur at the phase boundaries, thus exposing the impurities to the surface. Therefore, purification of crushed MG-Si by acid leaching is effective in removing metallic impurities. However, owing to the larger segregation coefficient of nonmetal impurities, such as nonmetal P, which usually exists as substituted silicon atoms or in the lattice space, the effect of acid leaching is not obvious, and other technological means are required to remove these impurities. Min and Sano[13] reported that calcium and phosphorus can form a stable compound Ca_3P_2, which can be effectively removed by acid leaching. Morita et al.[14] investigated the interaction parameter between calcium and phosphorus and the self-interaction parameter of phosphorus in molten silicon at 1723 K (1450 °C). The addition of calcium to silicon improved the subsequent removal of phosphorus during the acid leaching treatment, with a remarkably increase in the removal fraction. Johnston and Barati[15] studied the effect of calcium addition on the effect on removal of phosphorus, and it was found that the P concentration decreased with increasing quantities of added calcium. The most significant decrease took place when the quantity of added Ca increased from 2 to 3 pct, and the content of P in silicon decreased by two orders of magnitude when the quantity of added Ca was 4 pct. Meteleva-Fischer[16] determined that some impurity phases contain significant phosphorus content after alloying with calcium, which could be useful for the phosphorus removal. Li et al.[17] investigated the purification of MG-Si by solidification of a hypereutectic Al-Si melt with super gravity, with the refined silicon

being collected by aqua regia leaching. The mass fraction of P was reduced from 33.65 to 13.50 ppmw. Gumaste et al.[18] reported Al-Si solvent refining of MG-Si with a reduction of most of the metal impurities, and a reduction of the content of P from 45×10^{-6} to 15×10^{-6}. Hu et al.[19] studied the purification MG-Si by solvent refining and super gravity separation combined with acid leaching. The main impurities, including P, were efficiently removed by the Sn-Si process and acid leaching. Guo et al.[20] demonstrated that the concentrations of the main impurities, including P, and the typical metallic impurities, except for solvents Sn and Al were reduced to less than 1 ppmw through sequential Sn-Si and Al-Si refining processes after acid leaching. Li et al.[21] studied the effect of cooling rate on phosphorus removal during Al-Si solvent refining. They found that when the cooling rate decreases, the phosphorus removal rate increases. In 30 pct Si-Al alloy, when the cooling rate decreases from 32 to 0.55 mK s^{-1}, the phosphorus content decreases from 26 to 4.5 ppmw. Huang et al.[22] reported that the addition of copper increased the extraction yield of phosphorus from MG-Si from 23.2 to 42.2 pct. Chen et al.[23] reported that Ga-Si solvent refining could reduce the impurities elements, such as B and P. However, the removal fraction of P was only 14.84 pct when the Si proportion was 25 pct in the Ga-Si alloy.

Based on the above discussion, solvent refining and subsequent acid leaching can effectively improve the removal of phosphorus from MG-Si. However, all of these processes involved the addition of impurity elements. Furthermore, very little attention has been paid to the interaction between the position of phosphorus impurities in C-MG-Si and the acid leaching mechanism. In the present work, the effect of structural composition on the removal of phosphorus from MG-Si by acid leaching has been thoroughly analyzed. The evolution of the silicon microstructure before and after acid leaching using HCl and HCl–HF mixture was revealed and the influence of particle size, leaching time, temperature, and liquid–solid ratio on the acid leaching process was examined.

II. EXPERIMENTAL SECTION

A. Materials

Crude metallurgical-grade silicon (C-MG-Si) produced by the reduction of quartz in arc furnaces and secondary refined MG-Si (S-MG-Si) were obtained from commercial sources. The experimental procedure is depicted in Figure 1. The concentrations of impurities in the as-received MG-Si samples are listed in Table I. The block-shaped MG-Si feedstock was crushed and ground into powder. The ground particles were sieved in a standard testing sieve and silicon fractions with different particle sizes (<1000 μm) were collected. Five screens were used in the sieving stage, and consequently silicon powders with five different particle size fractions were collected. The size fractions and average particle sizes of the silicon powders used in the current work, as
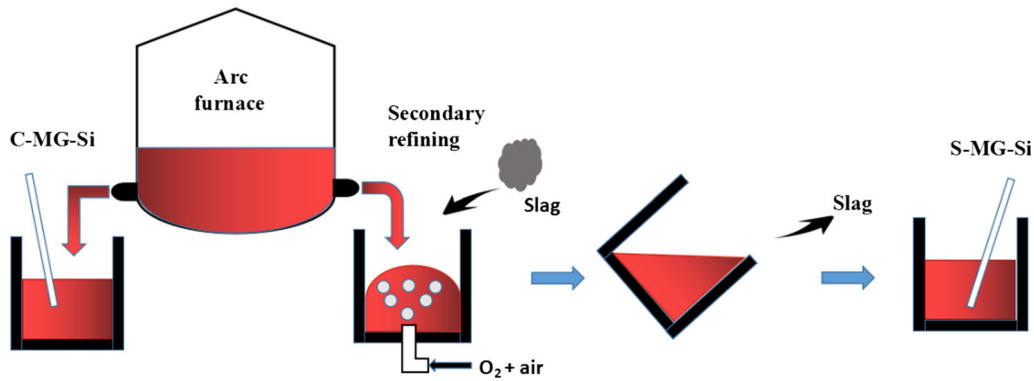
Fig. 1—Schematic of the experimental process.

Table I.   Content of Major Impurities in MG-Si (ppmw)

Type	Fe	Al	Ca	Mn	Ti	V	Cr	Ni	Cu	Zr	P
C-MG-Si	4225	6223	12291	348	376	476	98	367	85	22	85
S-MG-Si	4190	1230	283	124	239	395	68	288	62	13	76

Table II.   Size Fractions of Silicon Powders and the Corresponding Concentrations of Phosphorus Impurities

Sieve Mesh Size				
China Sieve (mesh)	(μm)	Average Particle Size (μm)	P in C-MG-Si (Ppmw)	P in S-MG-Si (Ppmw)
>200	<75	75	144	88
150–200	75–106	90.5	105	76
100–150	106–150	128	100	75
60–100	150–250	200	80	72
16–60	250–1000	625	75	69

well as the concentrations of phosphorus impurities are given in Table II.

When C-MG-Si was crushed and classified, P was segregated at the grain boundaries and the finer particles were enriched, but in S-MG-Si, the distribution of P in different particles was invariable. This phenomenon could be attributed to the difference in the composition and occurrence of phosphorus impurities in the MG-Si samples.

B. Acid Leaching

Each acid leaching experiment was carried out using 25 g of specimen in a beaker under constant stirring (600 rpm). At the end of each experiment, the solids were filtered and washed with distilled water before drying for analysis.

C. Characterization

The concentrations of impurities in MG-Si before and after acid leaching were determined by inductively coupled plasma (ICP) spectrometry. The microstructure of MG-Si and the composition of the precipitates were examined by scanning electron microscopy-energy dispersive spectroscopy (SEM-EDS) using an electron beam with an accelerating voltage of 30 kV and a beam current of 59 μA.

III.   RESULTS

A series of systematic leaching trails were performed to study the effect of particle size, time, temperature, and liquid–solid ratio on the degree of removal of phosphorus from MG-Si. The following results illustrate the main effects of each of these parameters.

A. Effect of Particle Size

MG-Si powders with five different particle size ranges were treated with 4.0 mol L^{-1} HCl at 338 K (65 °C) for 4 hours with a liquid/solid ratio of 4:1. The effect of particle size on the removal efficiency of phosphorus from C-MG-Si and S-MG-Si is shown in Figure 2. For C-MG-Si, the particle size has a significant effect on the dissolution of phosphorus. The efficiency of phosphorus removal is improved significantly as the particle size decreases, with over 52.1 pct of P leached when the particle size range was <75 μm. However, for S-MG-Si,
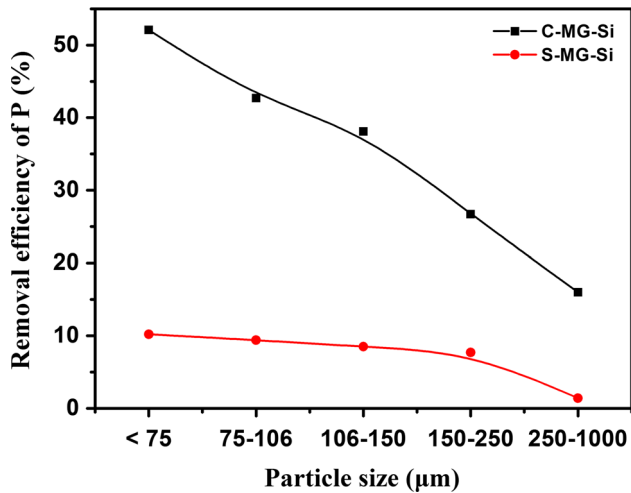
Fig. 2—Effect of particle size on the removal efficiency of P from MG-Si. Time: 4 h; temperature: 338 K (65 °C); initial acid concentration: 4.0 mol L^{-1}; liquid/solid: 4:1; stirring speed: 600 rpm.

Fig. 3—Effect of leaching time on the removal efficiency of P from MG-Si. Particle size: 75 to 106 μm; temperature: 338 K (65 °C); initial acid concentration: 4.0 mol L^{-1}; liquid/solid: 4:1; stirring speed: 600 rpm.

the particle size has little effect on the removal of phosphorus, and the removal rate was approximately 10 pct for all particle size ranges.

For C-MG-Si, the results indicated that more friable phases containing impurities were concentrated in the finer particle fractions during sieving. The proportion of finer particles in the C-MG-Si is very small, while the content of impurities in the finer particles is relatively high. Thus, finer silicon particles should be excluded from the acid leaching process to decrease the amount of impurities. Therefore, 75 to 106 μm was recommended as the optimal particle size for both C-MG-Si and S-MG-Si in the subsequent acid leaching process.

B. Effect of Leaching Time

To investigate the effect of leaching time on the removal efficiency of P, the leaching time was increased from 2 to 8 hours at 1-hour intervals, with the other leaching conditions kept as follows: particle size of 75 to 106 μm, 4.0 mol L^{-1} HCl, temperature of 338 K (65 °C), and a liquid/solid ratio of 4:1. The removal efficiency of P with increasing leaching time is shown in Figure 3. For C-MG-Si, the removal efficiency of P increased sharply in the initial stage of the leaching process, which can be attributed to the rapid reaction between the phosphorus-containing phase and HCl. Within 2 hours, 33.01 pct of phosphorus was extracted, and this value reached 50.49 pct after leaching for 6 hours. In contrast, in S-MG-Si, the removal efficiency of P was only 11.84 pct after leaching for 6 hours. There appeared to be no significant increase in the removal efficiency of P after 6 hours; consequently, 6 hours was recommended as the optimal leaching time for the following experiments.

C. Effect of Temperature

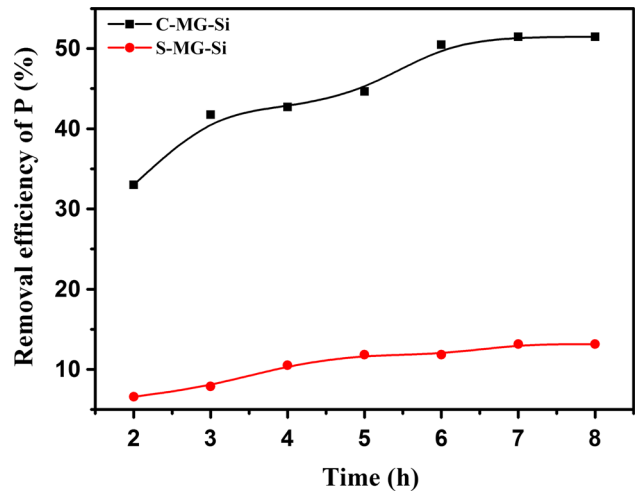The effect of temperature on the extraction yield of P was investigated by conducting experiments in the range

from 308 K to 348 K (35 °C to 75 °C); the other leaching conditions were maintained as follows: particle size of 75 to 106 μm, 4.0 mol L^{-1} HCl, leaching time of 6 hours, and a liquid/solid ratio of 4:1. The results presented in Figure 4 show that the removal efficiency of phosphorus impurities increased gradually with increasing temperature, with the maximum removal of 55.3 pct P in C-MG-Si and 21.1 pct P in S-MG-Si achieved at 348 K (75 °C). Taken into account that higher temperature will cause more acid solution loss, 338 K (65 °C) was recommended as the optimum temperature.

D. Effect of Liquid–Solid Ratio

The liquid–solid ratio is an important factor during the acid leaching process. A suitable liquid–solid ratio not only results in a more thorough reaction but also avoids leaching solution waste. The effect of the liquid–solid ratio on the removal efficiency of phosphorus impurities was studied in the liquid–solid range of 2:1 to 6:1, with the remaining leaching conditions kept constant. As shown in Figure 5, the removal efficiency of phosphorus increased with the increasing liquid–solid ratio. For C-MG-Si, a maximum removal efficiency of 54.3 pct P is obtained at a liquid–solid ratio of 6:1. For S-MG-Si, the removal efficiency of phosphorus in HCl solution was 3.95 pct at a liquid–solid ratio of 2:1, and increasing the liquid–solid ratio to 6:1 improved the removal efficiency to 19.74 pct, although the rate of improvement became very low as the liquid–solid ratio was increased. Thus, the optimum liquid–solid ratio was suggested to be 6:1.

E. Effect of Optimal Leaching Conditions on Phosphorus Removal

The optimum operation conditions for the removal of phosphorus from MG-Si are as follows: acid concentration: 4.0 mol L^{-1}, particle size of raw material 75 to
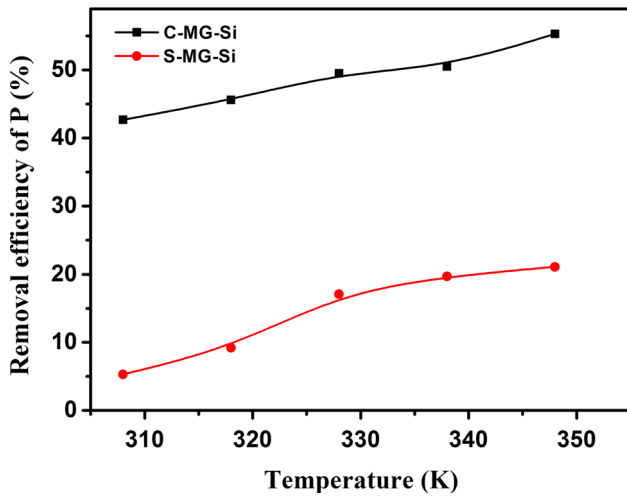
Fig. 4—Effect of leaching temperature on the removal efficiency of P from MG-Si. Particle size: 75 to 106 μm; time: 6 h; initial acid concentration: 4.0 mol L^{-1}; liquid/solid: 4:1; stirring speed: 600 rpm.

Fig. 6—Variation in phosphorus concentrations in MG-Si samples after leaching in HCl. Particle size: 75 to 106 μm; time: 6 h; temperature: 338 K (65 °C); initial acid concentration: 4.0 mol L^{-1}; liquid/solid: 6:1; stirring speed: 600 rpm.
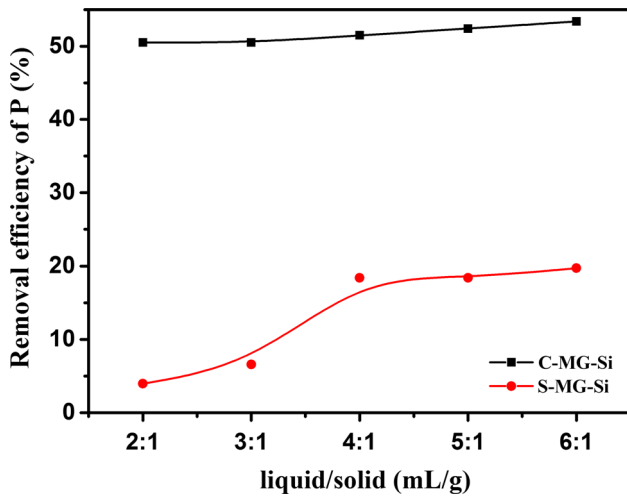

Fig. 5—Effect of liquid–solid ratio on the removal efficiency of P from MG-Si. Particle size: 75 to 106 μm; time: 6 h; temperature: 338 K (65 °C); initial acid concentration: 4.0 mol L^{-1}; stirring speed: 600 rpm.
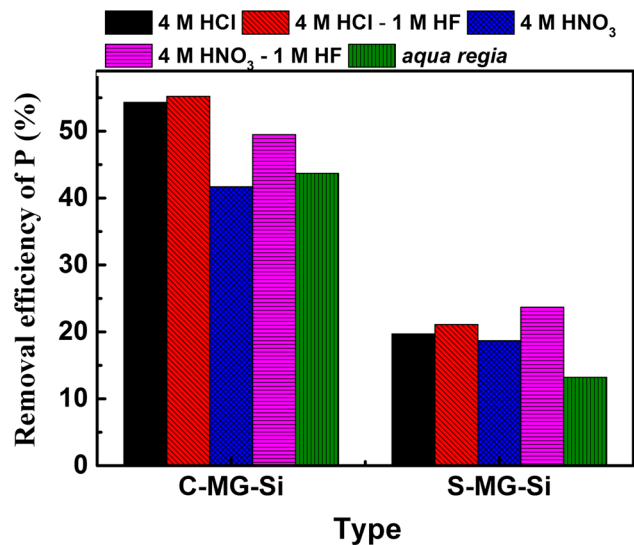
Fig. 7—Effect of different acid solution on the removal efficiency of P from MG-Si. Particle size: 75 to 106 μm; time: 6 h; temperature: 338 K (65 °C); liquid/solid: 6:1; stirring speed: 600 rpm.

106 μm, leaching time: 6 hours, leaching temperature: 338 K (65 °C), and liquid–solid ratio: 6:1. The content of P in MG-Si samples after acid leaching under these optimum conditions is shown in Figure 6.

The mass fraction of phosphorus in C-MG-Si was reduced from 105×10^{-6} to 48×10^{-6}, with the final removal efficiency of 54.3 pct, whereas the mass fraction of phosphorus in S-MG-Si was reduced from 76×10^{-6} to 61×10^{-6}, with a removal efficiency of only 19.7 pct. C-MG-Si is produced by the reduction of quartz in arc furnaces, without secondary refining in a ladle, which reduces the equipment utilized and the production costs.

F. Effect of Different Acid Solutions

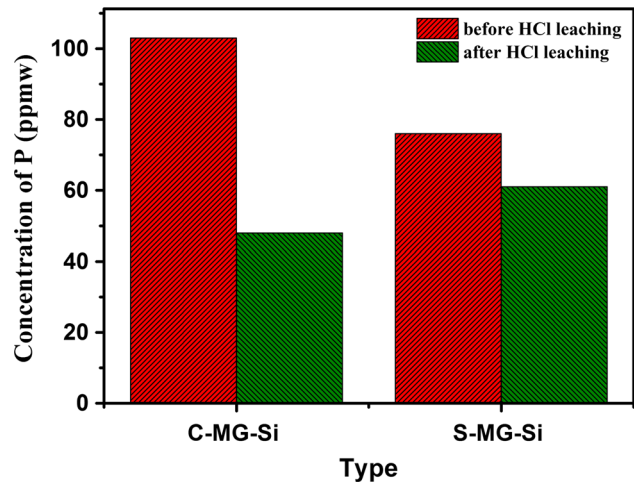Figure 7 shows the extraction of P in the C-MG-Si and S-MG-Si after various leaching agents. Compared

with nitrate, the structure of chloride ion in HCl acid is relatively simple, and the steric hindrance is smaller when it forms ligands with metal impurities, so the impurity removing effect is stronger than that of HNO$_3$ and aqua regia. Aqua regia has strong acidity and oxidization ability. So it can promote the leaching of metal impurities, its efficiency of removing impurity was second only to the HCl. The addition of HF to HCl or HNO$_3$, the removal rate of P was increased, which was mainly due to the high fluorine ion coordination and good coordination. Comparing the leaching effect of different acids on this two types of silicon, it can be found that the removal rules of phosphorus were basically the same, which shows that the sensitivity of impurity phase in acidic solvent plays a dominant role in the removal effect of impurities.

For the C-MG-Si, where the highest extraction was achieved when the sample was leached by 4.0 mol L^{-1} HCl to 1.0 mol L^{-1} HF, giving an extraction of 55.2 pct P; the removal effect was optimum under the condition of 4.0 mol L^{-1} HNO_3 to 1.0 mol L^{-1} HF leached for the sample of S-MG-Si, and the removal efficiency of P was 23.7 pct. The addition of HF-HCl resulted in improved extraction of phosphorus impurity. In order to ensure the preciseness of the contrast experiment, HCl-HF mixed acid was selected as the leaching agent to study the removal effect of metal impurities in silicon. The experimental study found that under the conditions of 4.0 mol L^{-1} HCl to 3.0 mol L^{-1} HF leaching, the removal of metal impurities in silicon to achieve the best results, as shown in Tables III and IV.

It was found that treatment by secondary refining resulted in lessening the extraction of most metal impurities from MG-Si as compared to that without secondary refined. The effect of addition of hydrofluoric acid to HCl on the purification of C-MG-Si is illustrated in Table III. It can be see that significantly better results could be attained through HCl-HF leaching than through HCl leaching. When the HCl-HF solution was applied, the concentration of all of the metal impurities decreased. The Fe concentration also decreased substantially, but remained at 363 ppmw owing to its high initial concentration (4225 ppmw). The extraction efficiency of Fe was 91.4 pct, this represents an improvement of at least 49.5 pct compared to the sample leached

by HCl. After leaching for 6 hours, the extraction efficiencies for Al, Ca, Mn, and Ti were 93.0, 99.1, 97.7, 96.0, and 98.1 pct, respectively. Furthermore, the Cr, Ni, Cu, and Zr impurities were removed efficiently to a final concentration lower than 1 ppmw; extraction efficiencies of 99.0, 99.7, 98.8, and 95.5 pct, respectively, were achieved. The extraction yield of impurities achieved using the HCl-HF solution was up to approximately 96.1 pct, the Si purity increased from 97.55 to 99.91 pct, while the extraction yield of impurities achieved using the HCl solution was approximately 83 pct.

As shown in Table IV, for the S-MG-Si leached with HCl-HF, most metal impurities can be reduced greatly. The extraction yield of impurities achieved using the HCl-HF solution was up to approximately 81.6 pct, the Si purity increased from 99.31 to 99.87 pct.

In summary, the HCl-HF mixed solution has better power to remove most impurities. This can be attributed to the strong corrosion of HF acid to the impurity phase in silicon and the synergistic impurity removal of HCl acid in the leaching process.

The obtained removal efficiency of phosphorus can be improved by adopting C-MG-Si as the raw material. Besides, the results suggested that adding HF acid was beneficial for the removal of most impurities. The feasibility of this method was confirmed experimentally, and these results provided a new reference for the study of solar-grade silicon production by pre-treating MG-Si with hydrometallurgy method.

Table III. Content and Removal Efficiencies of Impurities in the C-MG-Si After Acid Leaching by 4.0 mol L^{-1} HCl and 4.0 mol L^{-1} HCl to 3.0 mol L^{-1} HF mixture (Particle Size: 75 to 106 μm; Time: 6 h; Temperature: 338 K (65 °C); Liquid/Solid: 6:1; Stirring Speed: 600 rpm)

Impurity Elements	C-MG-Si (Ppmw)	HCl (Ppmw)	Removal Efficiency (Pct)	HCl-HF (Ppmw)	Removal Efficiency (Pct)
Fe	4225	2303	45.5	363	91.4
Al	6223	628	89.9	435	93.0
Ca	12291	259	97.9	112	99.1
Mn	348	47	86.5	8	97.7
Ti	376	334	11.2	15	96.0
V	476	432	9.2	9	98.1
Cr	98	67	31.6	<1	99.0
Ni	367	88	76.0	<1	99.7
Cu	85	4	95.3	<1	98.8
Zr	22	6	72.7	<1	95.5

Table IV. Content and Removal Efficiencies of Impurities in the S-MG-Si After Acid Leaching by 4.0 mol L^{-1} HCl and 4.0 mol L^{-1} HCl to 3.0 mol L^{-1} HF Mixture (Particle Size: 75 to 106 μm; Time: 6 h; Temperature: 338 K (65 °C); Liquid/Solid: 6:1; Stirring Speed: 600 rpm)

Impurity Elements	S-MG-Si (Ppmw)	HCl (Ppmw)	Removal Efficiency (Pct)	HCl-HF (Ppmw)	Removal Efficiency (Pct)
Fe	4190	3161	24.6	667	84.1
Al	1230	737	40.1	436	64.6
Ca	283	114	59.7	56	80.2
Mn	124	98	21.0	19	84.7
Ti	239	216	9.6	13	94.6
V	395	368	6.8	23	94.2
Cr	68	51	25.0	17	75.0
Ni	288	147	49.0	24	91.7
Cu	62	9	85.5	4	93.5
Zr	13	8	38.5	1	92.3

IV. DISCUSSION

A. Microstructure of the C-MG-Si

Figures 8(a) and (b) present the microstructure of C-MG-Si and the distribution of representative impurity elements, respectively, as detected by SEM-EDS. C-MG-Si, which was not treated by secondary refining, results in significant difference in optical appearance in comparison to the S-MG-Si, especially when it comes to the amount and structure of inclusions (Figure 8(a)). It can be observed that well-divided homogeneous layers of various impurity phases were contained in the inclusions, which indicates better segregation of impurity phases. This result is consistent with the influence of calcium addition on the microstructure of MG-Si.[16]

Furthermore, the chemical composition of the impurity phases of C-MG-Si, which was not treated by secondary refining, was also significantly different from those of S-MG-Si, which was treated by secondary refining. The impurity phases detected in C-MG-Si are presented in Table V. Compared with the microstructure of the S-MG-Si, the Si-Ca phase became the
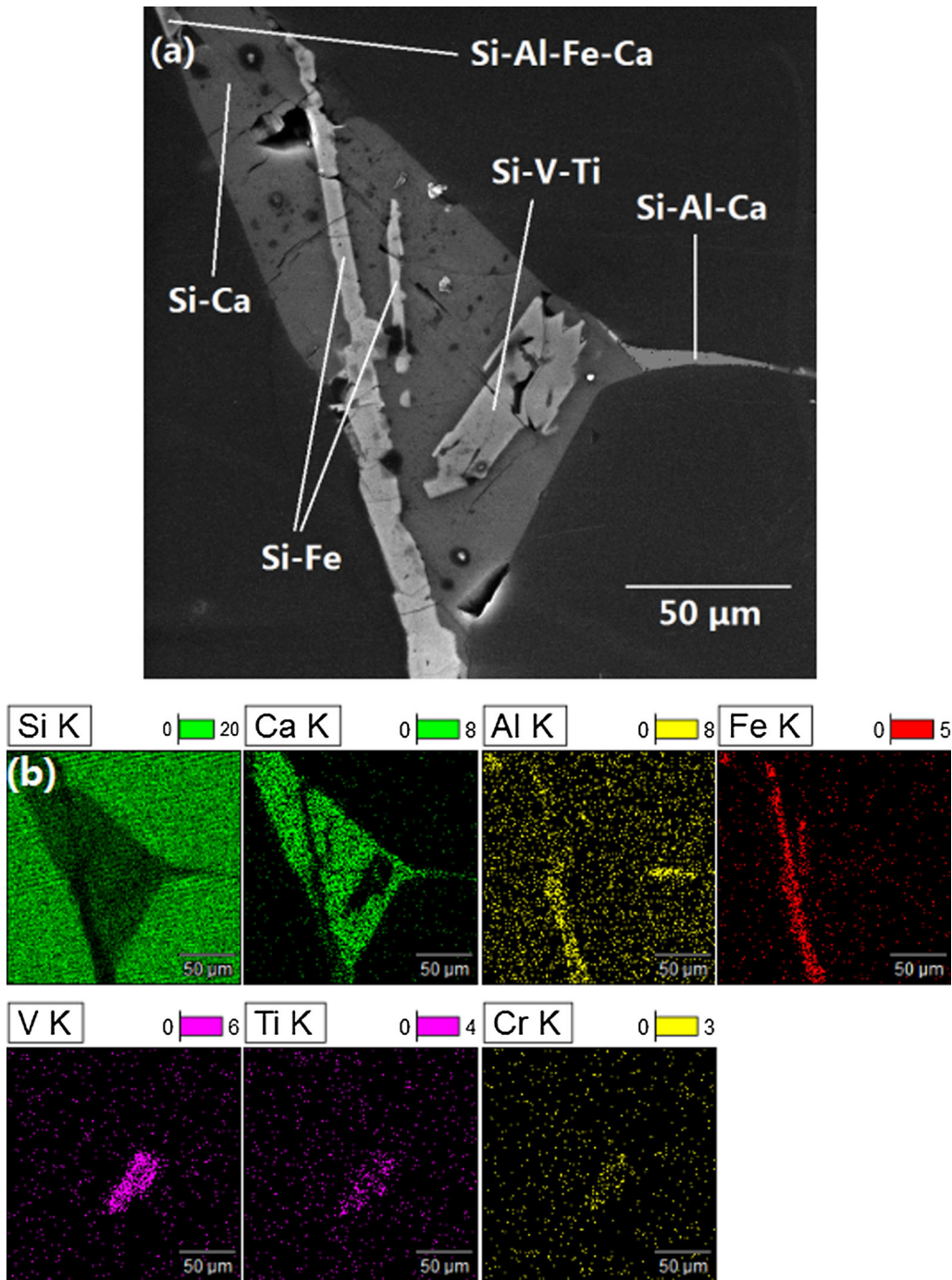

Fig. 8—Microstructure of C-MG-Si. (a) SEM image and (b) EDS spectral mapping of impurity phases.

dominant phase in the impurity inclusions of C-MG-Si. Based on the Ca-Si binary phase diagram, in the composition of 90 to 97 wt pct Si-rich alloy, only one eutectic point is formed between $CaSi_2$ and Si at 1297 K (1024 °C)[24] Thus, $CaSi_2$ was generated during the solidification of the molten silicon.

In the impurity inclusions, a new Si-Al-Ca phase was observed with a composition close to that of a reported Si_2Al_2Ca phase,[25] which was the only phase containing phosphorus (Figure 8(a); Table V). The Si_2Al_2Ca phase shows an affinity for phosphorus, with up to 0.53 wt pct dissolved in this phase. This result is similar to that reported in the literature,[26] in which phosphorus is only detected in the Si_2Al_2Ca phase. Thus, the removal efficiency of phosphorus would be increased if the Si_2Al_2Ca phase were leached out. A Si-Al-Fe-Ca phase was also observed, usually located next to the major $CaSi_2$ phase, which may be attributed to iron dissolution in the Si-Al-Ca phase. Shimpo et al.[14] reported

phosphorus dissolution in the $CaSi_2$ phase, but no phosphorus content was detected in this phase in the present work. One possible reason for this difference is that the source of silicon used in the previous study was doped with 3 wt pct phosphorus.

B. Influence of Acid Treatment on the Microstructure of C-MG-Si

The sensitivity of the precipitates in C-MG-Si to acid was investigated by observing the microstructures of C-MG-Si before and after the addition of HCl. Figure 9 reveals the microstructural evolution of C-MG-Si after leaching with HCl. The phosphorus-containing phase (Si_2Al_2Ca) was dissolved after exposure to HCl. Moreover, only a Si-Fe phase remained on the surface of the cavity after HCl exposure (Figures 9(a, b)), indicating that the insoluble phases, such as Si-V-Ti, can be removed together with the leachable Si-Ca, Si-Al-Ca,

Table V. Chemical Composition of the Main Precipitates in C-MG-Si, Wt Pct

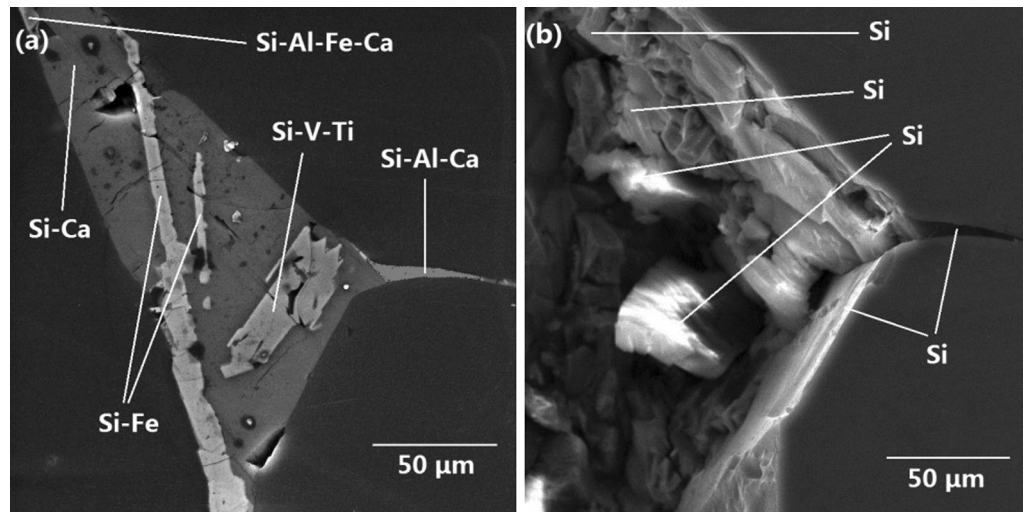|	Phase	Si	Fe	Al	Ca	Mn	V	Other
1	Si-Al-Fe-Ca	35.73	32.05	21.76	8.37	0.77		1.32 (Ni)
2	Si-Ca	57.22		0.82	41.96			
3	Si-Fe	51.34	43.96	2.17	1.78	0.75		
4	Si-V-Ti	51.30	1.16		0.36		40.77	6.41 (Ti)
5	Si-Al-Ca	41.19		34.14	24.14			0.53 (P)

Fig. 9—Microstructural evolution of C-MG-Si after etching: (a) initial microstructure and (b) after exposure to 4.0 mol L^{-1} HCl; temperature: 338 K (65 °C); time: 1 h.

Table VI. Chemical Composition of Main Precipitates in C-MG-Si After Exposure to 4.0 mol L^{-1} HCl, Wt Pct [Time: 1 h; Temperature: 338 K (65 °C)]

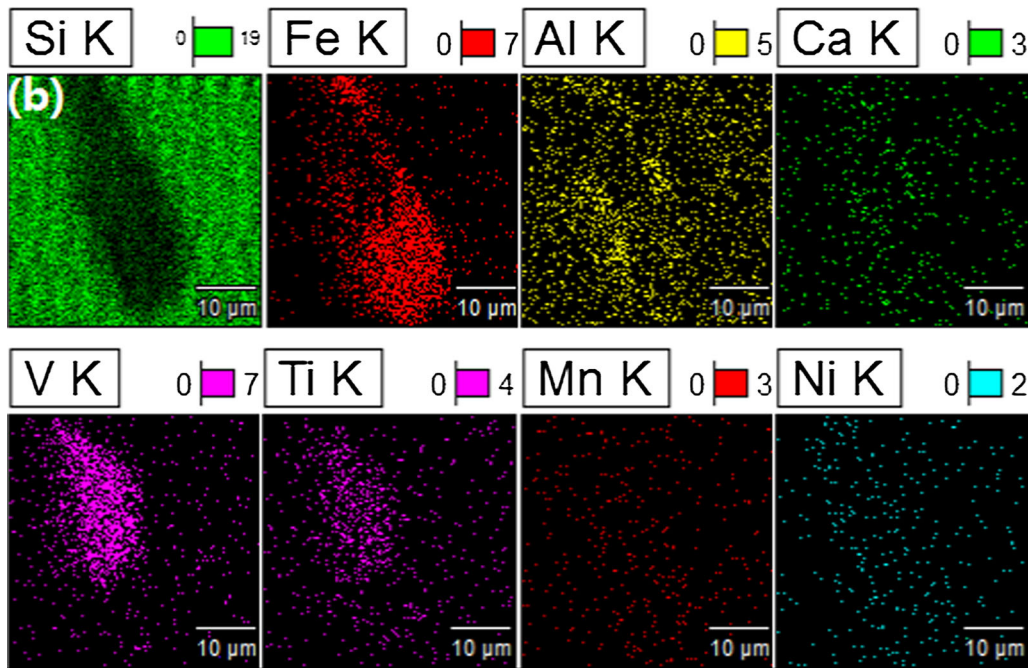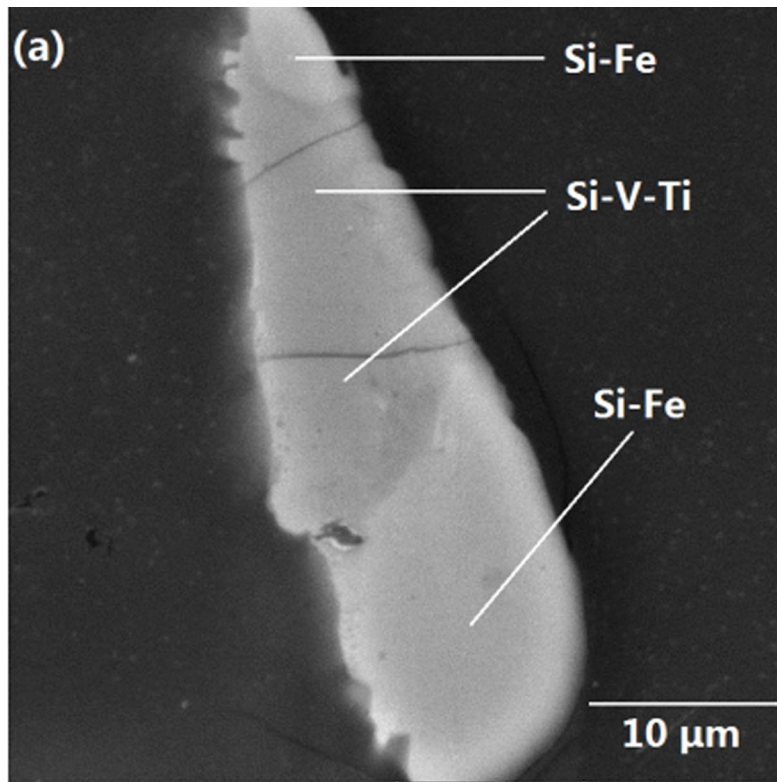|	Phase	Si	Fe	Al	Ca	Mn	V
1	Si-Fe	54.33	36.86	4.78	2.27	1.16	0.59
2	Si	92.07	2.82	1.39	3.72		
3	Si	100					
4	Si	96.30		1.04	2.66		
5	Si	99.24			0.76		

Fig. 10—Microstructure of S-MG-Si. (*a*) SEM image and (*b*) EDS spectral mapping of impurity phases.

Table VII. Chemical Composition of Main Precipitates in S-MG-Si, Wt Pct

	Phase	Si	Fe	Al	Ca	Ni	Mn	Ti	V
1	Si-Fe	54.40	36.58	4.94	0.69	1.02	0.77	0.45	1.15
2	Si-V-Ti	51.38	3.93	0.66			1.39	7.46	35.18
3	Si-Fe	53.07	41.43	3.68		0.77	1.05		

and Si-Al-Fe-Ca phases. This phenomenon may be the result of some insoluble silicide precipitation phases embedded in the soluble silicide phases, as demonstrated in Figure 9(a). Consequently, some unleachable silicide phases may be removed from the silicon surface when the leachable phases are dissolved. However, as these phases are difficult to separate from the upgraded silicon, the purity of silicon will not be improved by this mechanism. According to Margarido et al.,[27] the reactivity order of these precipitated phases in HCl is as follows:

$$CaSi,\ CaSi_2,\ CaAl_2Si_{1.5} > Caalsifer > Al-Fe-Si >> FeSi_2.$$
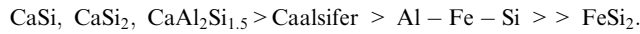
This result indicates that the dissolution rates of Si-Ca-based alloys in HCl are much higher than that of $FeSi_2$ in HCl.

As shown in Table VI, some metallic impurities remain after leaching with HCl at 338 K (65 °C) for 1 hour, which can probably be attributed to an insufficient leaching time.

C. Microstructure of the S-MG-Si

The typical microstructure of S-MG-Si and the composition of the precipitation phases were detected by SEM-EDS, and the corresponding results are presented in Figure 10 and Table VII. As shown in Figure 8(a), different-colored impurities indicated different phases composed of different crystal structures and impurity contents. The chemical compositions of the main impurity phases in S-MG-Si can be divided into two categories, indicated by the dark gray and light gray areas. The dark gray area can be seen as a Si-V-Ti-rich phase, as the content of vanadium was very high (>35 wt pct), the content of silicon was greater than 51 wt pct, and the content of titanium was greater than 7 wt pct. The light gray area can be regarded as a Si-Fe-rich alloy, as the content of Fe was greater than 26 wt pct and the content of Si was greater than 67 wt pct. The detection of the Si-V-Ti phase indicates the tendency of titanium to be present in high content in phases with V and Si. The observation of the Si-Fe and Si-V-Ti phases in S-MG-Si confirms the high stability of these phases during secondary refining treatment.

Figure 10(b) reveals the distribution of the representative impurity elements such as iron, aluminum, manganese, vanadium, titanium, calcium, and nickel. The distribution pattern of Fe is almost identical to the shape of the light gray area and the boundary is clear, which indicates that Fe is mainly concentrated in the Si-Fe phase. However, although phosphorus is distributed evenly in the silicon matrix, phosphorus can barely be detected in the impurity inclusions owing to the low sensitivity of EDS to phosphorus. This

Table VIII. Chemical Composition of Main Precipitates in S-MG-Si After Exposure to 4.0 mol L^{-1} HCl, Wt Pct [Time: 6 h; Temperature: 338 K (65 °C)]

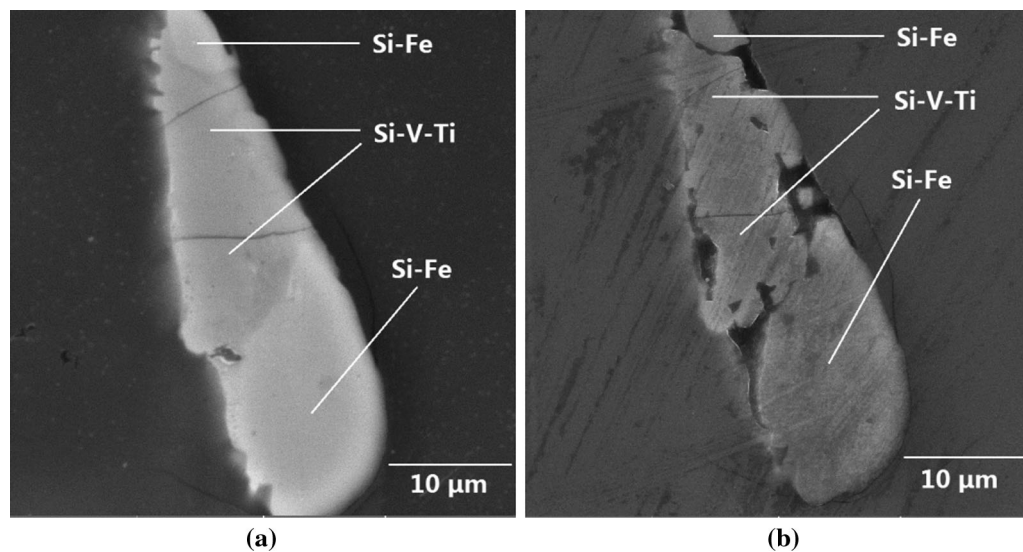|	Phase	Si	Fe	Al	Ca	Ni	Mn	Ti	V
1	Si-Fe	64.07	29.03	3.93	0.58	1.05	0.83		0.52
2	Si-V-Ti	50.42	4.57	0.88			1.15	8.52	34.46
3	Si-Fe-Al	54.88	21.84	10.58	2.86	2.13	0.71	2.14	4.86
4	Si-Fe	55.94	38.21	3.78		1.03	1.04		

(a)   **(b)**

Fig. 11—Microstructural evolution of S-MG-Si after etching: (a) initial microstructure and (b) after exposure to 4.0 mol L^{-1} HCl; temperature: 338 K (65 °C); time: 1 h.
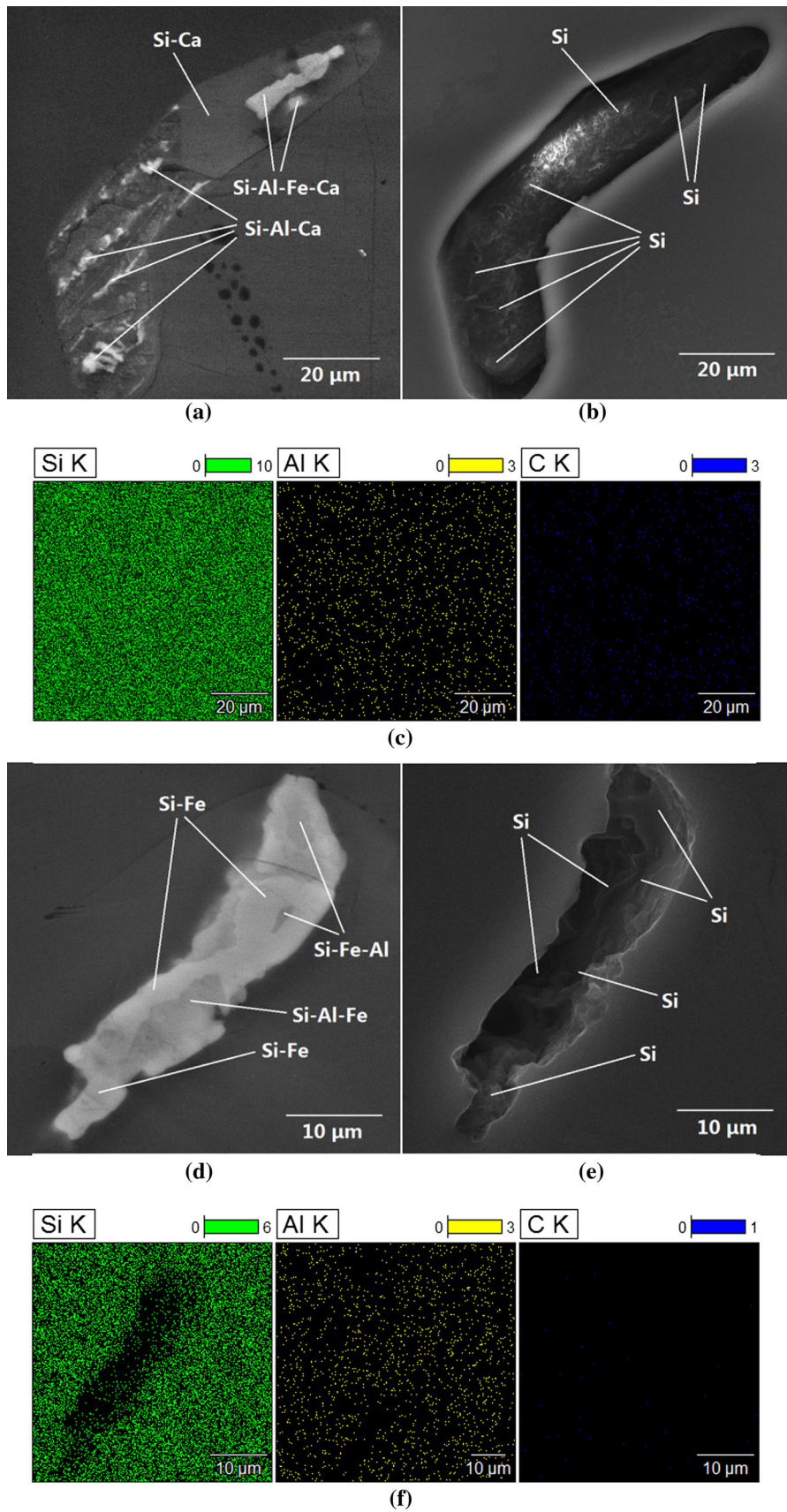
Fig. 12—Microstructural evolution of MG-Si after etching: (a) initial microstructure of C-MG-Si; (b) after exposure to 4.0 mol L^{-1} HCl to 3.0 mol L^{-1} HF; (c) elements EDS spectral mapping of impurity phase after exposure to HCl to HF; (d) initial microstructure of S-MG-Si; (e) after exposure to 4.0 mol L^{-i} HCl to 3.0 mol L^{-1} HF; (f) elements EDS spectral mapping of impurity phase after exposure to HCl-HF; temperature: 338 K (65 °C); time: 6 h.

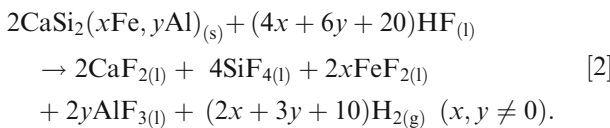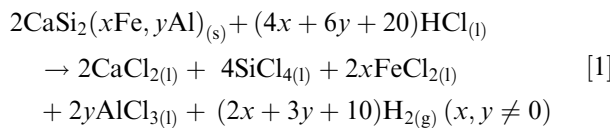distribution indicates that phosphorus cannot be efficiently removed from S-MG-Si by acid leaching alone.

D. *Influence of Acid Treatment on the Microstructure of S-MG-Si*

The sensitivity of the precipitates in S-MG-Si to acid was studied by observing the microstructures of the samples before and after exposure to HCl. The microstructural evolution of S-MG-Si after etching with HCl is presented in Figure 10 and the chemical compositions of the main precipitates after HCl exposure are shown in Table VIII. As shown in Figures 11(a) and (b), the Si-Fe, Si-V-Ti, and Si-Fe-Al phases are practically insoluble in HCl, which is quite consistent with the results reported by Margrido.[28]

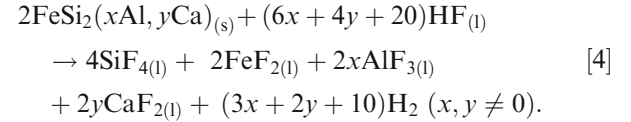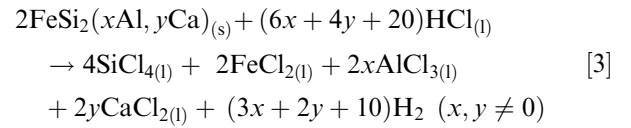### E. *Micro-Structural Evolution of MG-Si under HCl-HF etchant*

Some metallic impurities still remain after etching with HCl at 338 K (65 °C) for 1 hour (see Figure 9). Because of the corrosion time is too short, metal impurities cannot be completely dissolved, so we choose 6 hours as the corrosion time. The microstructural evolution of MG-Si before and after etching with HCl-HF lixiviant is presented in Figure 12. As shown in Figures 12(b) and (e), the phases, including Si-Ca, Si-Fe, Si-Fe-Al, Si-Al-Ca, and Si-Al-Fe-Ca, are soluble, as evidenced by the holes left on the surface. Most of the precipitates are removed owing to the attack of HCl-HF mixtures. However, according to the EDS mapping analysis results, a small amount of Al still remained in silicon after exposure to the HCl-HF mixture, while only a small amount of carbon was distributed sporadically in both C-MG-Si and S-MG-Si after exposure to the HCl-HF mixture.

The dissolution of metal impurities present in the precipitated phase of C-MG-Si, such as Fe, Al, and Ca by leaching with HCl-HF can be expressed by the following equations:

$$2CaSi_2(xFe, yAl)_{(s)} + (4x + 6y + 20)HCl_{(l)}$$
$$\rightarrow 2CaCl_{2(l)} + 4SiCl_{4(l)} + 2xFeCl_{2(l)} \qquad [1]$$
$$+ 2yAlCl_{3(l)} + (2x + 3y + 10)H_{2(g)} \ (x, y \neq 0)$$

$$2CaSi_2(xFe, yAl)_{(s)} + (4x + 6y + 20)HF_{(l)}$$
$$\rightarrow 2CaF_{2(l)} + 4SiF_{4(l)} + 2xFeF_{2(l)} \qquad [2]$$
$$+ 2yAlF_{3(l)} + (2x + 3y + 10)H_{2(g)} \ (x, y \neq 0).$$

After secondary refining treatment, the reaction mechanism of metal impurities Fe, Al, Ca from S-MG-Si in HCl-HF solution could be described by Eqs. [3] and [4]:

$$2FeSi_2(xAl, yCa)_{(s)} + (6x + 4y + 20)HCl_{(l)}$$
$$\rightarrow 4SiCl_{4(l)} + 2FeCl_{2(l)} + 2xAlCl_{3(l)} \qquad [3]$$
$$+ 2yCaCl_{2(l)} + (3x + 2y + 10)H_2 \ (x, y \neq 0)$$

$$2FeSi_2(xAl, yCa)_{(s)} + (6x + 4y + 20)HF_{(l)}$$
$$\rightarrow 4SiF_{4(l)} + 2FeF_{2(l)} + 2xAlF_{3(l)} \qquad [4]$$
$$+ 2yCaF_{2(l)} + (3x + 2y + 10)H_2 \ (x, y \neq 0).$$

Equations [1] and [2] explain that $CaSi_2$, Si_2Al_2Ca, and Si-Al-Fe-Al phases dissolved in HCl-HF mixture, while Eqs. [3] and [4] indicate that $FeSi_2$ and Si-Fe-Al phases were eliminated by HCl-HF.

V. CONCLUSIONS

The effect of structural composition and impurity content on the removal of phosphorus from MG-Si by HCl leaching was investigated. SEM results indicate that the segregation of impurity phases in C-MG-Si was better than that in S-MG-Si. The Si-Fe, Si-Fe-Al, and Si-V-Ti phases were insoluble in HCl, but the Si-Ca, Si-Al-Ca, and Si-Al-Fe-Ca phases were completely dissolved in of HCl. The only phosphorus-containing phase detected was the soluble Si-Al-Ca phase; hence, the removal of phosphorus can be enhanced by acid leaching. Moreover, the influences of particle size, reaction time, temperature, and liquid–solid ratio on the removal efficiency of phosphorus was studied. The optimum operating conditions for HCl leaching are as follows: raw material of 75 to 106 μm, time of 6 hours, and temperature of 338 K (65 °C), acid concentration of 4 mol L^{-1}, and liquid–solid ratio of 6:1. The removal efficiencies of phosphorus impurities from C-MG-Si and S-MG-Si were up to 54.3 and 19.7 pct, respectively. Therefore, the content of phosphorus in silicon can be effectively reduced with the acid leaching method by adopting C-MG-Si as the raw material.

Besides, it was found that treatment by secondary refining resulted in lessening the extraction of most metal impurities from MG-Si as compared to that without secondary refined. After 6 hours of leaching MG-Si with a mixture composed of 4.0 mol L^{-1} HCl and 3 mol L^{-1} HF, the purity of C-MG-Si and S-MG-Si were increased from 97.55 and 99.31 pct to 99.91 and 99.87 pct, respectively, with extraction efficiencies of 96.1 and 81.6 pct, respectively. The etching results showed that the leaching behavior of impurity inclusions strongly depended on the composition of the major

impurities. HCl-HF mixture was an effective lixiviant for dissolving impurity inclusions in both C-MG-Si and S-MG-Si.

ACKNOWLEDGMENTS

REFERENCES

1. L.A.V. Teixeira and K. Morita: *ISIJ*, 2009, vol. 49, pp. 783–87.
2. J. Li, L. Zhang, Y. Tan, D. Jiang, D. Wang, and Y. Li: *Vacuum*, 2014, vol. 103, pp. 33–37.
3. M. Xiaodong, Z. Jian, and T. Wang: *Rare Met.*, 2009, vol. 28, pp. 221–25.
4. S.S. Zheng, T.A. Engh, M. Tangstad, and X.T. Luo: *Sep. Purif. Technol.*, 2011, vol. 82, pp. 128–37.
5. M.A. Martorano, J.B.F. Neto, T. S. Oliveira, and T. OTsubaki: *Mater. Sci. Eng. B*, 2011, vol. 176B, pp. 217–26.
6. N.P. Tucker: *Iron. Steel Inst.*, 1927, vol. 15, pp. 412–14.
7. J. Dietl: *Sol. Cells*, 1983, vol. 10, pp. 145–54.
8. I.C. Santos, A.P. Gonçalves, C.S. Santos, M. Almeida, M.H. Afonso, and M.J. Cruz: *Hydrometallurgy*, 1990, vol. 23, pp. 237–46.
9. C.E. Norman, E.M. Absi, and R.E. Thomas: *Can. J. Phys.*, 2011, vol. 63, pp. 859–62.
10. S.K. Sahu and E. Asselin: *Hydrometallurgy*, 2012, vol. 121, pp. 120–25.
11. R. Zeng, Y.H. Wang, J.X. Zhang, J.Q. Xu, H.Y. Li, and X.F. Chen: *Adv. Mater. Res.*, 2012, vol. 549, pp. 428–31.
12. H. Zhang, Z. Wang, W. Ma, K. Xie, and L. Hu: *Ind. Eng. Chem. Res.*, 2013, vol. 52, pp. 7289–96.
13. D.J. Min and N. Sano: *Metall. Mater. Trans. B*, 1988, vol. 19B, pp. 433–39.
14. T. Shimpo, T. Yoshikawa, and K. Morita: *Metall. Mater. Trans. B*, 2004, vol. 35B, pp. 277–84.
15. M.D. Johnston and M. Barati: *Sep. Purif. Technol.*, 2013, vol. 107, pp. 129–34.
16. Y.V. Meteleva-Fischer, Y. Yang, R. Boom, B. Kraaijveld, and H. Kuntzel: *Intermetallics*, 2012, vol. 25, pp. 9–17.
17. L. Jing-Wei, Z.C. Guo, H.Q. Tang, Z. Wang, and S.T. Sun: *Trans. Nonferrous Met. Soc. China*, 2012, vol. 22, pp. 958–63.
18. B.C. Mohanty and R.K. Galgali: *Sol. Energy Mater.*, 1987, vol. 16, pp. 289–96.
19. L. Hu, Z. Wang, X. Gong, Z. Guo, and H. Zhang: *Sep. Purif. Technol.*, 2013, vol. 118, pp. 699–703.
20. L. Hu, Z. Wang, X. Gong, Z. Guo, and H. Zhang: *Metall. Mater. Trans. B*, 2013, vol. 44B, pp. 828–36.
21. Y. Li, B. Ban, J. Li, T. Zhang, X. Bai, and J. Chen: *Metall. Mater. Trans. B*, 2015, vol. 46B, pp. 542–44.
22. L. Huang, H. Lai, C. Lu, M. Fang, W. Ma, and P. Xing: *Hydrometallurgy*, 2016, vol. 161, pp. 14–21.
23. J. Li, B. Ban, Y. Li, X. Bai, T. Zhang, and J. Chen: *Silicon*, 2017, vol. 9, pp. 77–83.
24. H. Okamoto: *J. Phase Equilib. Diffus.*, 2007, vol. 28, p. 404.
25. F. Margarido, M.O. Figueiredo, A.M. Queiróz, and J.P. Martins: *Ind. Eng. Chem. Res.*, 1997, vol. 36, pp. 5291–95.
26. J.C. Anglezio, C. Servant, and F. Dubrous: *J. Mater. Res.*, 1990, vol. 5, pp. 1894–99.
27. F. Margarido, M.H. Bastos, M.O. Figueiredo, and J.P. Martins: *Mater. Chem. Phys.*, 1994, vol. 38, pp. 342–47.
28. F. Margarido, J.P. Martins, M.O. Figueiredo, and M.H. Bastos: *Hydrometallurgy*, 1993, vol. 34, pp. 1–11.